Metallophysics and Advanced Technologies
Металофіз. новітні технол.
Metallofiz. Noveishie Tekhnol.
2024, vol. 46, No. 7, pp. 663–677
https://doi.org/10.15407/mfint.46.07.0663
Reprints available directly from the publisher

PACS numbers: 06.60.Vz, 61.72.Ff, 62.20.Qp, 81.20.Vj, 81.30.Kf, 81.40.Ef, 81.70.Bt

Effect of Heat Input During Welding on the Microstructure and Mechanical Properties of the Heat-Affected Zone of MIL-A-46100 Armour Steel

O. A. Slyvins'kyy, V. V. Kvasnyts'kyy, I. A. Vladymyrskyi,
S. P. Bisyk*, Ye. P. Chvertko, and V. L. Kovalenko

National Technical University of Ukraine
'Igor Sikorsky Kyiv Polytechnic Institute',
57 Beresteiskyi Ave.,
UA-03056 Kyiv, Ukraine
**National Defence University of Ukraine,*
28 Povitrianykh Syl Ave.,
UA-03049 Kyiv, Ukraine

The paper presents the results of studies concerning the influence of the heat input of gas metal arc welding on the microstructure and mechanical properties of the metal of the heat-affected zone (HAZ) of a high-hardness armour plate made according to MIL-A-46100. Using the bead test method, the heat input is varied in the range of 0.9–2.2 kJ·mm^{-1}, and the distribution of microhardness inside the metal of the welded samples, the microstructure, and the impact toughness of the HAZ sections are investigated. The studied steel reveals a high sensitivity to welding heat. According to the microhardness distribution, the entire metal of the HAZ, the width of which increased from ≅ 25.0 to 28.0 mm with increasing heat input in the studied range of values, is characterized by a lower hardness compared to the base metal. As established, the lowest impact toughness is observed in the metal directly adjacent to the weld of the overheating zone, which undergoes complete austenization, grain enlargement, and further transformation of austenite with the formation of lath martensite and bainite sheaves' mixture under the influence of the welding thermal cycle. An increase in the heat input is accompanied by

Corresponding author: Oleksiy Anatoliyovych Slyvins'kyy
E-mail: o.slyvinsky@gmail.ua

Citation: O. A. Slyvins'kyy, V. V. Kvasnyts'kyy, I. A. Vladymyrskyi, S. P. Bisyk, Ye. P. Chvertko, and V. L. Kovalenko, Effect of Heat Input During Welding on the Microstructure and Mechanical Properties of the Heat-Affected Zone of MIL-A-46100 Armour Steel, *Metallofiz. Noveishie Tekhnol.*, **46**, No. 7: 663–677 (2024). DOI: 10.15407/mfint.46.07.0663

a decrease in the martensitic component and, accordingly, an increase in the bainite fraction in the metal of this part of the HAZ. In turn, this leads to the impact toughness enhancement, but only for the values of welding heat input of 0.9, 1.1, and 1.3 kJ·mm^{-1}. In the case of heat input of 2.2 kJ·mm^{-1}, at which the metal of the overheated area underwent the most significant softening, its impact toughness was significantly lower compared to the case of welding with lower heat-input values and 30% lower than that of the base metal. This effect can be explained by a modification in the morphology of the carbide component of the bainite phase, with the gradual replacement of lower bainite by upper bainite, as well as the release of boron-containing carbide particles along the boundaries of primary grains due to excessive slowing of metal cooling in the overheated area. Thus, welding of the studied steel using parameters ensuring high deposition rate with a heat input of about 2.2 kJ·mm^{-1} can cause resistance degradation of the metal of the HAZ to brittle fractures under the influence of dynamic loads, providing a negative impact on the ballistic resistance and durability of its welded joints.

Key words: high-hardness armour steel, gas metal arc welding, heat-affected zone, microstructure, microhardness, impact toughness.

В роботі представлено результати досліджень впливу погонної енергії дугового зварювання топкою електродою у захисному газі на мікроструктуру та механічні властивості металу зварювальної зони термічного впливу (ЗТВ) броньової криці високої твердости, виготовленої за ТУ MIL-A-46100. Використовуючи методу валикової проби, погонну енергію варіювали в інтервалі значень 0,9–2,2 кДж·мм$^{-1}$, досліджували розподіл мікротвердости в металі зварних зразків, мікроструктуру та показники ударної в'язкости ділянок ЗТВ. Досліджена криця виявила високу чутливість до зварювального тепла. Відповідно до розподілу мікротвердости, весь метал зони термічного впливу, ширина якої зі зростанням погонної енергії в досліджуваному інтервалі значень збільшилася від близько 25,0 до 28,0 мм, має нижчі значення твердости, ніж основний метал. Встановлено, що найнижчі показники ударної в'язкости має метал безпосередньо прилеглої до шва ділянки перегріву, який під впливом термічного циклу зварювання зазнає повної аустенізації, укрупнення зерна та подальшого перетворення аустеніту з формуванням суміші рейкового мартенситу та пакетного бейніту. Зростання погонної енергії супроводжується зменшенням мартенситної складової та, відповідно, зростанням частки бейніту в металі цієї ділянки ЗТВ. В свою чергу це спричиняє збільшення ударної в'язкости, але тільки для значень погонної енергії у 0,9, 1,1 та 1,3 кДж·мм$^{-1}$. У випадку погонної енергії зварювання у 2,2 кДж·мм$^{-1}$, за якої метал ділянки перегріву зазнавав найістотнішого знеміцнення, його ударна в'язкість виявилася значно меншою, ніж для зварювання з меншими значеннями погонної енергії, та на 30% меншою, ніж у основного металу. Подібний ефект можна пояснити зміною морфології карбідної складової бейнітної фази з поступовим заміщенням нижнього бейніту верхнім, а також виділенням вздовж меж первинних зерен частинок борвмісних карбідів через надмірне уповільнення охолодження металу ділянки перегріву. Таким чином, зварювання дослідженої криці на форсованих режимах з погонною енергією біля 2,2 кДж·мм$^{-1}$ може спричиняти деґрадацію

опірности металу ЗТВ щодо крихких руйнувань під впливом динамічних навантажень, що матиме неґативний вплив на балістичну стійкість і живучість її зварних з'єднань.

Ключові слова: броньова криця високої твердости, зварювання топкою електродою у захисному газі, зона термічного впливу, мікроструктура, мікротвердість, ударна в'язкість.

(Received 19 July, 2024; in final version, 24 July, 2024)

1. INTRODUCTION

To date, high-hardness armour steels (HHAS) according to MIL-A-46100 with a thickness of 3–20 mm are widely used in the manufacture of welded hulls and turrets of light armoured fighting vehicles (AFVs) with ballistic protection against small arms bullets and small calibre projectiles [1]. In the state after quenching and low-temperature tempering to a hardness of *HB* 4.77–5.34 GPa, these materials must meet the requirements of ballistic resistance (resistance to penetration and piercing under high-speed impact loads), durability (ability to resist brittle fracture under repeated impact and explosive loads), processability, and weldability [2].

The required set of properties, with a limited carbon content ($\leq 0.32\%$ wt.) due to welding requirements, is provided by the Cr–Ni–Mo alloying system, microalloying with strong carbide-forming elements (V, Nb, Ti) and minimizing the concentration of impurities [1, 3]. In turn, to achieve maximum hardness and maintain a sufficient level of toughness, the HHAS rolling technology involves the introduction of high-temperature thermomechanical controlled processing (TMCP) and rapid heat treatment by hardening, allowing an effective control of the grains structure and dispersion of the carbide phase [2, 4]. To implement high-speed quenching in the rolling mill, flow and efficient use of alloying elements, boron microalloying is used. It is known that the increase in steel hardenability is due to the ability of boron segregated along the austenite grain boundaries to prevent the formation of ferrite phase nuclei [5, 6]. According to Ref. [7], the effect of 0.001–0.003% wt. B on steel hardenability is equivalent to adding 0.6% wt. Mn + 0.7% wt. Cr + 0.5% wt. Mo, or 1.5% wt. Ni to its composition. Since the beneficial effect is realized exclusively by boron atoms dissolved in the matrix and not bound in non-metallic inclusions, its maximum content in high-strength quenched and tempered steels is limited to 0.005% wt. and 0.02–0.05% wt. Al and 0.02–0.05% wt. Ti are added to their composition [7, 8].

The most common welding method used in the production of lightweight AFVs is gas metal arc welding (GMAW) using low-carbon high-alloyed electrode wires of the Cr–Ni–Mn system. This makes it possible

to obtain an austenitic–ferritic structure in the weld with high ductility and durability under impact loads applied outside the welded joints, and not to use preheating and post-weld tempering to prevent cold cracks [9]. Since the strength and hardness of the weld metal (WM) formed in this way are significantly lower than those of the base metal (BM), the required level of ballistic protection could be achieved by the design of the welded components.

In contrast to WM, changes in mechanical properties caused by structural and phase transformations in the adjacent heat affected zone (HAZ) cannot be compensated by appropriate alloying through welding materials, since the metal in this zone is not melted, but only heated to various temperatures. Austenization and tempering are the key processes in the formation of the HAZ metal properties of armour steels, as well as for any other high-strength quenched and tempered steels. According to the heating–cooling conditions, four typical regions of HAZ are distinguished (Fig. 1): coarse-grained HAZ (CGHAZ), fine-grained HAZ (FGHAZ), intercritical HAZ (ICHAZ), and subcritical HAZ (SCHAZ).

The most critical effects on the quality and serviceability of HHAS welded joints are the weakening of SCHAZ metal, reducing its ballistic resistance compared to BM [12, 13], and causing an embrittlement and a tendency to slow fracture of CGHAZ metal due to the enlargement of its grain structure and repeated quenching [9, 14]. At the same time, the effect of the structure, hardness and strength of CGHAZ metal due to it on its performance under pulsed impact loads is ambiguous. On

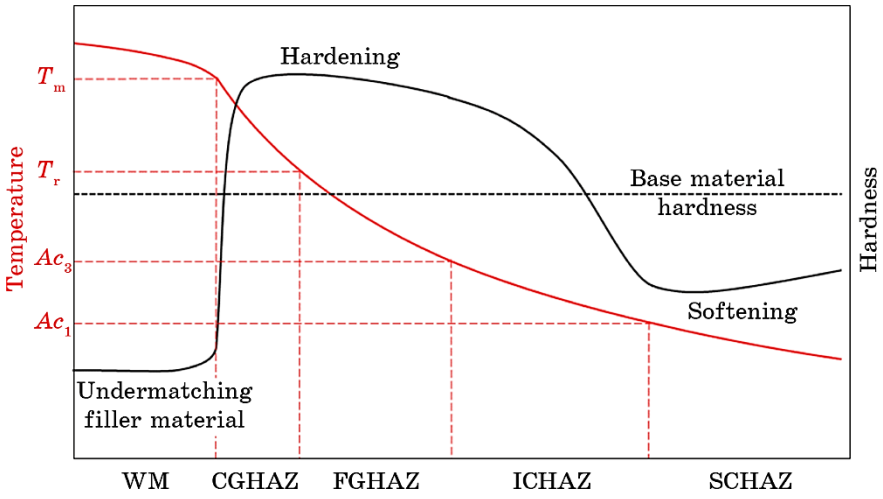

Fig. 1. Peak temperature and hardness profile of welded quenched and tempered steel, schematic adapted from Refs. [10–12]: T_m is melting point; T_r is temperature of the beginning of the collective recrystallization.

the one hand, for the material of an armour barrier with a hardness in the range of 4.50–5.60 GPa, there is a directly proportional relationship between the hardness value and the resistance to penetration of armour-piercing ammunition [15, 16]. In particular, in Ref. [11], it was shown that the relationship between the hardness of the HAZ metal and its dynamic compressive strength under deformation with a rate of $3 \cdot 10^3$ s^{-1} can be characterized by a linear regression equation:

$$\sigma = 3.21 HV_{10} + 439.07, \quad (1)$$

where σ—dynamic compressive strength, MPa, HV_{10}—hardness of the welded joint metal measured by Vickers approach with a load on the indenter of 98.1 N within the range 220–470 HV_{10}.

On the other hand, as shown in Ref. [17] on the example of *T*-shaped and *L*-shaped welded substructures, under conditions of impact loads applied outside WM and HAZ, the initiation of brittle fracture occurs in the CGHAZ metal near WM due to the localization of the plastic deformation and the low ductility of the CGHAZ metal.

The penetration of high-hardness thin sheet armour occurs by the mechanism of 'hard plugging' under the so-called adiabatic shear, caused by the localization of plastic deformation in an extremely narrow micron-wide region. The metal in this region is intensively heated by the heat generated during plastic deformation, but does not have time to spread throughout the target volume [18, 19]. In turn, it is the structural factor providing a decisive influence on the material's resistance to deformation localization. In particular, according to Ref. [2], for steels with final structure formed by martensitic transformation, strain localization occurs in the areas of the hardest structural components, such as carbide particles or transformation twins. Moreover, in Ref. [20], it was shown that the size ratio of martensite packages and carbide particles has the most significant effect on the brittle strength of these steels.

Given that structural–phase transformations in HAZ metal occur under non-equilibrium conditions of the welding thermal cycle, which 'erases' the structure created by TMCP and changes the set of BM properties, optimization of the welding parameters determining the permissible values range of the HAZ metal cooling time is a relevant fundamental and technological issue. The minimum permissible values of the cooling time at austenite transformation start temperatures of 800–500°C are chosen to prevent excessive quenching and cold crack formation within CGHAZ, and the maximum permissible values of the cooling time are set to prevent excessive weakening of SCHAZ metal. The welding heat input (see Eq. (2)) has a direct impact on the cooling time of the welded joint metal sections, the value of which also determines the width of the HAZ, its individual sections and the depth of penetration.

The objective of the present study is to investigate the microstructural and mechanical properties under dynamic loading of HAZ metal in MIL-A-46100 armour steel under study, and to determine the effect of welding heat input on the performance of welded joints made of this material.

2. RESEARCH MATERIAL AND METHODOLOGY

Experiments were based on the bead-on-plate test. GMAW bead deposition was performed on plate 8 mm thick. Chemical composition of the base metal and electrode wire of 1.2 mm are summarized in Table 1.

As a protective gas, a mixture 98% Ar + 2% CO_2 was used. Welding parameters are listed in Table 2. The welding was performed with 'Jäckle ProPULS 400' automatic welder, stabilization of welding speed was ensured by 'ESAB Miggytrac B501' tractor.

The dimensions of the plates, the design of the welding tooling, and the sequence of beads' deposition prevent the outside influence on the free cooling of the HAZ metal. Samples for further studies of structural, microhardness, and impact bending tests were cut in a direction perpendicular to the axes of the welded beads (Fig. 2) by waterjet method preventing additional thermal effects on the material.

Welding heat input, Q, and time of cooling from 800 to 500°C, $t_{8/5}$, were determined using methodology ISO TR 17671 for the case of 3-dimensional heat flow during welding of semi-infinite workpiece:

TABLE 1. Chemical composition (% wt.) of the investigated steel and filer metal.

C	Si	Mn	P	S	Cr	Ni	Mo	V	Al	Ti	Cu	B
Base metal: MIL-A-46100 Armour Steel												
0.27	0.31	1.19	0.006	0.001	0.41	0.06	0.083	0.012	0.032	0.037	0.014	0.0019
Filler metal: ESAB OK Outrod 16.95												
0.07	0.80	6.90	0.020	0.010	18.7	8.20	0.20	–	–	–	0.20	–

TABLE 2. GMA welding process parameters (* is shown calculated values).

No. of bead run	Welding current I, A	Arc voltage U, V	Welding speed υ, mm·s^{-1}	Heat input Q, kJ·mm^{-1}	Cooling time from 800 to 500°C $t_{8/5}$, s	Time above temperature 1000°C $t_{>10}$, s
1	185	18.3	3.0	0.9*	4.8*	3.1*
2	200	20.8	3.0	1.1*	5.8*	3.7*
3	210	22.9	3.0	1.3*	6.9*	4.4*
4	295	28.4	3.0	2.2*	11.6*	7.5*

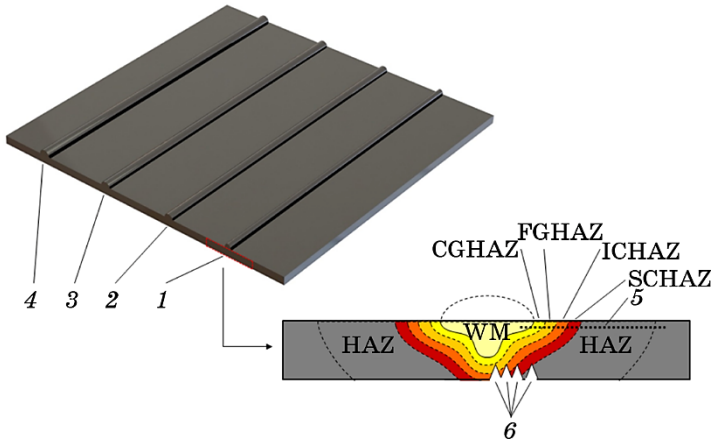

Fig. 2. Scheme of GMAW bead deposition and sample preparation for microhardness measurements and Charpy impact tests: surfacing beads (*1*)–(*4*), microhardness measuring direction (*5*), notches positions (*6*).

$$Q = 0.8\frac{UI}{\upsilon}10^{-3}, \tag{2}$$

$$t_{8/5} = (6700 - 5T_0)Q\left(\frac{1}{500 - T_0} - \frac{1}{800 - T_0}\right), \tag{3}$$

where U—arc voltage, V, I—welding current, A, υ—welding speed, mm·s^{-1}, T_0—initial plate temperature (20°C).

Time above temperature 1000°C, $t_{>10}$, was determined for the CGHAZ metal with maximum temperature of 1350°C using Eq. (4) [21]:

$$t_{>10} = 0.07\frac{2Q}{\lambda(1350 - T_0)}, \tag{4}$$

where λ—average thermal conductivity coefficient of the studied steel within the range of temperature values of 1000–1350°C ($\lambda = 31.0$ J·m^{-1}·s^{-1}·K^{-1}). Parameter $t_{>10}$ serves as a conditional indicator of the primary grain structure enlargement of CGHAZ metal as a result of the collective recrystallization process. However, the exact value of the complete dissolution temperature of fine-dispersed phases, capable of blocking the migration of the intergranular boundaries, depends on the chemical composition of the steel under study and may slightly exceed 1000°C.

It is worth noting that the use of austenitic filler metal for welding of high-hardness armour steels is a required step aimed at minimizing

the risk of cold cracks formation. This creates certain difficulties when setting the rational welding parameters, since high-alloyed austenitic-electrode wire has a significantly lower thermal conductivity and lower melting point compared to BM. In turn, the thermal power of the arc is often not enough to ensure proper penetration of the parts being joined. In particular, welding of 6–8 mm thick parts using parameters corresponding to the beads 1–3 (Table 2) is possible only with double-sided butt welds, with a gap between the parts of at least 2.5–3 mm. For similar conditions, a single-pass butt weld requires significantly more powerful welding parameters with a heat input corresponding to the bead 4 (Table 2).

The microstructure of the samples was studied using a Neophot-32 optical microscope and a TESCAN VEGA3 scanning electron microscope (SEM).

Microhardness analysis was performed using a Leco M-400 tester with a load of 1.96 N (200 g). The distribution of microhardness was determined in the cross-section of the samples, at a distance of 1.5 mm from the face surface of the plate, on which the beads were deposited (Fig. 2). The distance between adjacent points at which the microhardness was determined was 0.25 mm.

Impact bending tests were performed at room temperature using a KM-30 pendulum test rig with 55×7.5×8 mm samples having 2 mm high V-shaped concentrator cut. The concentrator cuts were made from the side opposite to the deposition face, and their tops were consistently located near the metal of the test areas: CGHAZ, FGHAZ, ICHAZ, and SCHAZ, respectively, as shown in Fig. 2. To compensate the influence of possible structural microinhomogeneities, the impact strength of each area was determined by averaging the results of three tests.

3. RESULTS AND DISCUSSION

The microhardness distribution in the studied samples with beads deposited using parameters 1–4 (Table 2) fits into the general trend: with an increase in the heat input, the width of the HAZ and all its typical areas increases, while the minimum hardness is observed in the transition region between ICHAZ and SCHAZ. In turn, the softening degree of the metal in this HAZ region does not depend on the heat input value, but is determined by the alloying of the steel. For comparison, the microhardness distribution in the HAZ of the beads deposited with heat input of 0.9 and 2.2 kJ·mm^{-1} is shown in Fig. 3.

Given the economical alloying of the studied steel, in particular, the low total content of Mo, V, and Si, which can increase resistance to tempering during heating [22], the recovery of microhardness to the BM level, which averages to 488 $HV_{0.2}$, occurs at a considerable distance from the fusion line. The total width of the HAZ increased from

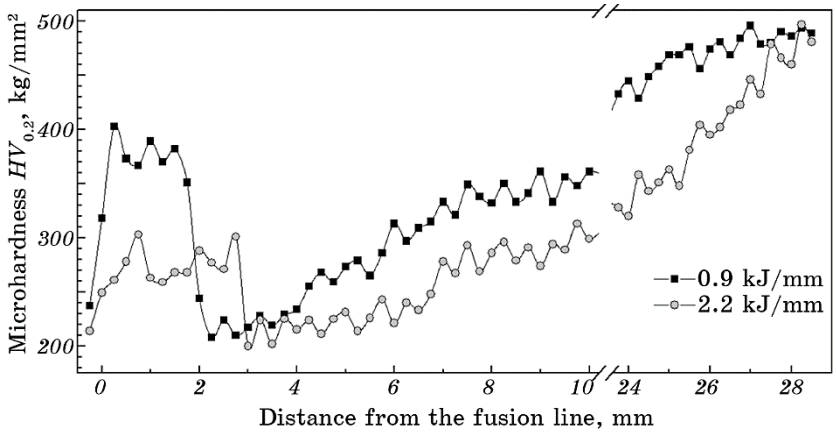

Fig. 3. Microhardness profiles of the heat-affected zones of the beads deposited on MIL-A-4610 steel plate with heat input of 0.9 and 2.2 kJ·mm^{-1}.

≅ 25.0 to 28.0 mm with heat-input increase from 0.9 to 2.2 kJ·mm^{-1}.

As can be seen, the HAZ areas that underwent austenization during heating (CGHAZ and FGHAZ) did not harden to BM level during cooling from the maximum temperatures: the maximum determined hardness of the CGHAZ metal for heat input of 0. 9 kJ·mm^{-1} is of 403 $HV_{0.2}$, and 303 $HV_{0.2}$ for 2.2 kJ·mm^{-1}. This may be due to the relatively low (as for armour steels) content of carbon and hardenability-enhancing elements (Mn, Ni, Mo). Thus, under the conditions of high-speed quenching due to the specifics of welding thermal cycles, there is no formation of a structure with hardness higher than that of BM in the areas of HAZ adjacent to the fusion line, as observed in HHAS with a higher content of carbon and solid solution strengthening elements [12].

The impact bending test results received on 3 specimens from each HAZ area formed during bead deposition with heat input of 0.9 kJ·mm^{-1} is shown in Fig. 4. With increase of the distance from the fusion line, the values of impact work KV gradually increase. At the same time, the sample with the concentrator applied in the CGHAZ metal has the lowest impact toughness, even compared to the high-hardness quenched BM. Therefore, further experiments on the effect of welding heat input on the degradation of the HAZ mechanical properties were conducted for this particular area. The impact test results of the CGHAZ metal of samples 1–4 (Table 2) are shown in Fig. 5.

It can be seen that an increase in the heat input from 0.9 to 1.3 kJ·mm^{-1}, which was accompanied by a decrease in the maximum microhardness of the CGHAZ metal from 403 to 333 $HV_{0.2}$, has an inverse effect on its impact toughness. That is, lower metal hardness corresponds to higher values of impact work KV (Fig. 5). However, in the case of the highest heat input of 2.2 kJ·mm^{-1}, at which the CGHAZ

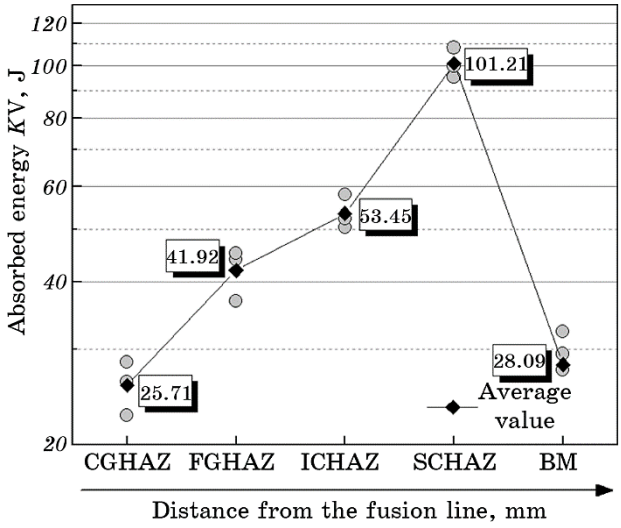

Fig. 4. Charpy impact energy measured at room temperature for HAZ areas of sample 1 (Table 2).

metal of the studied steel underwent the most significant softening, the impact work was significantly lower compared to the welding with lower heat input and 30% lower compared to BM (19.59 J *vs*. 28.09 J).

The results of optical-microscopy studies revealed that BM has a fine-grained martensitic–bainitic structure with a predominance of the

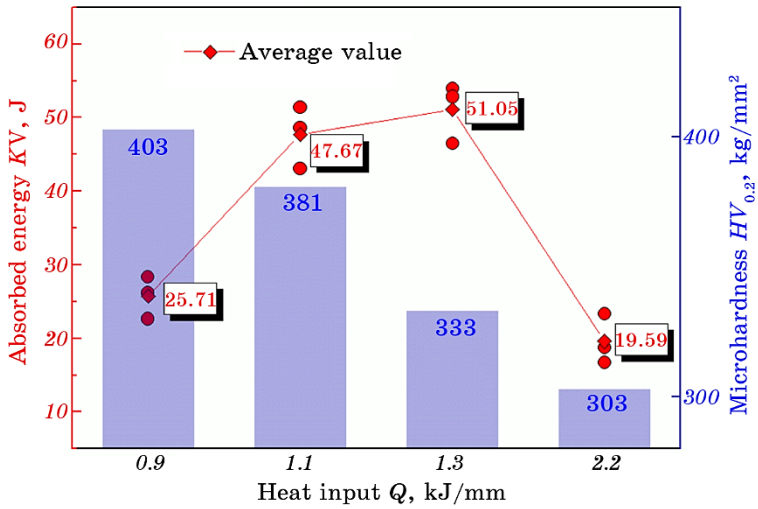

Fig. 5. Charpy impact energy data at the temperature of +20°C and maximum microhardness values in CGHAZ of samples 1–4 (Table 2).

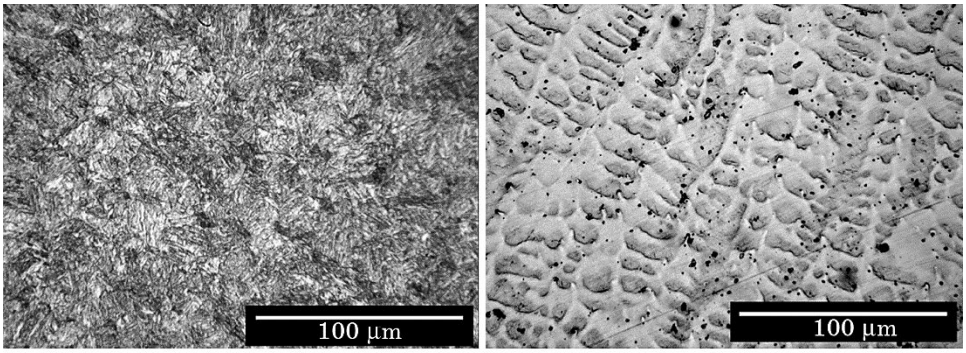

Fig. 6. Microstructure of BM (*a*) of investigated MIL-A-46100 high-hardness armour steel and WM (*b*) after bead deposition.

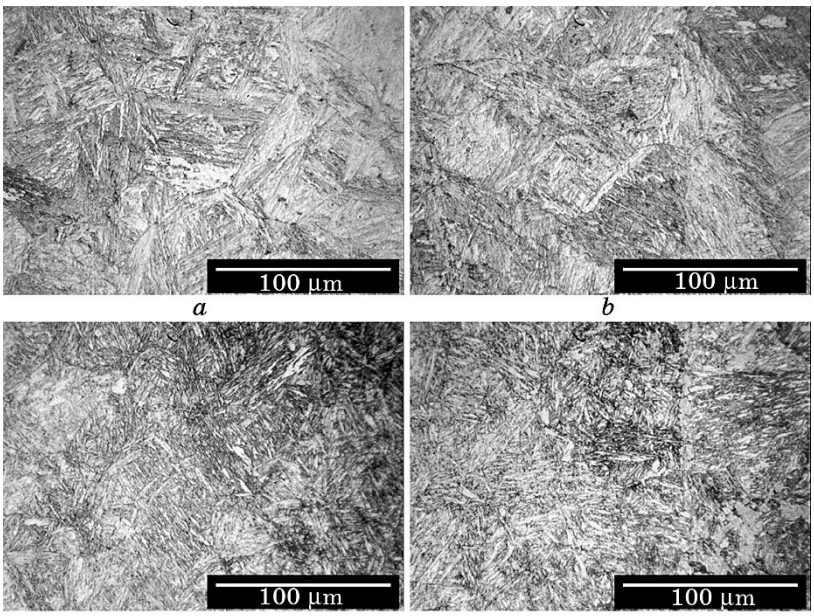

Fig. 7. Microstructure of CGHAZ of investigated MIL-A-46100 high-hardness armour steel after bead deposition with heat input of: 0.9 kJ·mm^{-1} (*a*), 1.1 kJ·mm^{-1} (*b*), 1.3 kJ·mm^{-1} (*c*), 2.2 kJ·mm^{-1} (*d*).

martensitic component (Fig. 6, *a*). In turn, the austenitic structure of WM with a cellular–dendritic form of crystallites (Fig. 6, *b*) is due to the used electrode wire (Table 1).

The final structure of the CGHAZ metal (Fig. 7) of all studied samples was formed by the shear mechanism of austenite transformation.

In contrast to the background of the enlarged primary grains typical for BM, a needle-like microstructure of lath martensite and bainite sheaves mixture is observed. With an increase in the heat input, the bainite fraction in the metal of these areas increases, so, the CGHAZ of samples 3 and 4 ($Q = 1.3$ and 2.2 kJ·mm^{-1}, respectively) demonstrates a predominantly bainitic structure.

Figure 8 shows a comparison of SEM images of the CGHAZ microstructure in the samples 1 and 4 ($Q = 0.9$ and 2.2 kJ·mm^{-1}, respectively). It can be seen that, despite the increase in the time of the metal remaining at the temperatures of the development of collective recrystallization in the studied areas of the CGHAZ ($t_{>10}$ increased from 3.1 to 7.5 s), the average primary grains size was changed insignificantly. Taking into account the chemical composition of the steel, this is probably due to the blocking the migration of intergranular boundaries by carbides or carbonitrides of titanium and vanadium. Within the CGHAZ, the grain size reaches a maximum of 70–80 μm for the sample 1, and 90–100 μm for the sample 4. Obviously, such a slight enlargement of the grain structure cannot cause a sharp decrease in the impact strength of the CGHAZ metal of the sample 4.

It is worth noting that due to the specific shape of the penetration of the bead test specimens and the corresponding configuration of the HAZ (Fig. 2), regardless of the location of the notch, during the impact bending tests, only crack initiation and development occurred in the controlled zone, while the fracture area spread to other parts of the

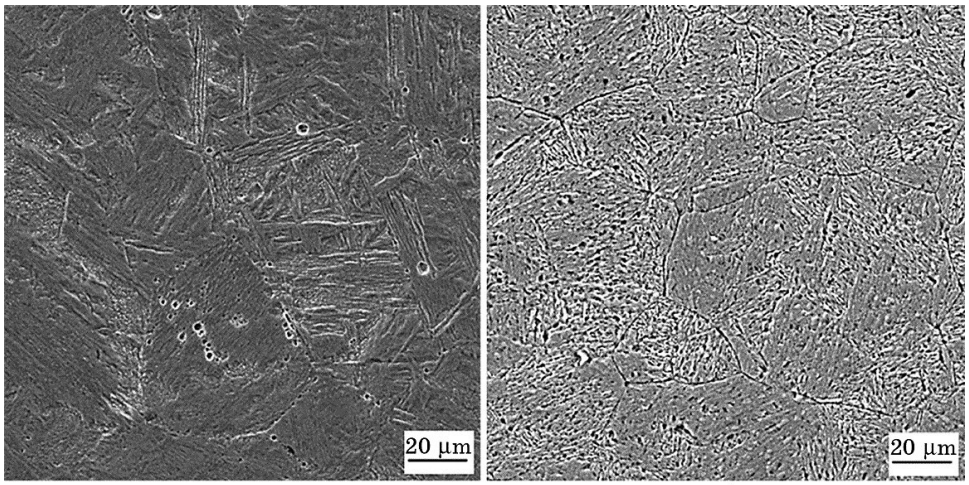

Fig. 8. SEM images of the CGHAZ microstructure after bead deposition with heat input of 0.90 kJ·mm^{-1} (*a*) and 2.2 kJ·mm^{-1} (*b*); SEM HV: 20.0 kV, SEM magnification: 3700.

HAZ or even along the WM. Thus, the obtained results characterize the ability of the metal in the studied areas to resist fracture initiation but do not allow assessing its resistance to fracture development. Nevertheless, they make it possible to differentiate clearly the brittle strength of individual HAZ areas under dynamic loading. Since impact toughness characterizes the resistance of a material to local plastic deformations concentrated in small volumes around stress concentrators, it is the most structure-dependent mechanical characteristic, which, in addition to grain size, is significantly influenced by the size and morphology of non-metallic inclusions and dispersed phase emissions.

The effect of welding heat input on the CGHAZ microstructure established in this study is quite typical for welding of high-strength quenched and tempered steels. An increase in heat input causes an increase in time of cooling from 800 to 500°C $t_{8/5}$, which also leads to an increase in the bainite fraction in the martensitic–bainitic structure of CGHAZ metal. In Ref. [23], it was shown for steel S1100Q that increase in $t_{8/5}$ leads to modification of the carbide component and bainite phase morphology, with the gradual replacement of lower bainite by upper one. In turn, the authors of Ref. [24] explain the sharp decrease in the impact toughness in the case of prolonged cooling in the temperature range of 800–500°C by the presence of the upper bainite dominant structure with coarse particles of the carbide phase in CGHAZ metal.

Another reason for the degradation of the impact toughness of CGHAZ metal after welding with a heat input of $Q = 2.2$ kJ·mm^{-1} may be associated with the release of carbide-phase particles along the primary grains boundaries. According to the results of in-depth studies [25] of boron-containing steel, a decrease in the cooling rate from the temperature of complete austenization and, accordingly, an increase in the cooling duration, reduce the segregation amplitude of boron along austenite grain boundaries due to the precipitation of boron carbides at the boundaries, as this precipitation depletes the boron content. In turn, as established in [6], the extensive precipitation of borocarbides results in lower notch hardness.

Thus, the results of the present study indicate that the use of welding parameters with increased deposition rate and a heat input of $\cong 2.2$ kJ·mm^{-1} for the studied steel, although it allows increasing the process productivity and reducing the total welding time, causes an excessive reduction in the brittle strength of CGHAZ metal. In turn, this effect will adversely affect the performance of welded joints under high-speed shock-wave loads.

4. CONCLUSIONS

1. The dependences of the microhardness and impact toughness of HAZ of

MIL-A-46100 high hardness armour steel on the heat input of gas metal arc welding (GMAW) in the range of 0.9–2.2 kJ·mm^{-1} were obtained.

2. Under the influence of GMAW thermal cycles, the studied steel showed a high tendency to softening. In particular, even the area of the HAZ metal that undergoes austenization during heating does not harden to the BM 488 $HV_{0.2}$ hardness level after cooling: the maximum determined hardness of the HAZ metal for heat input of 0.9 kJ·mm^{-1} is 403 $HV_{0.2}$, and for 2.2 kJ·mm^{-1}—303 $HV_{0.2}$.

3. Within the HAZ, the lowest impact strengths are found in the metal of coarse-grained regions (CGHAZ), the structure of which consists of a lath martensite and bainite sheaves mixture.

4. According to the impact bending tests results, an increase in heat input from 0.9 to 1.3 kJ·mm^{-1}, accompanied by a decrease in the martensitic component fraction and, accordingly, an increase in the proportion of bainite in CGHAZ metal, causes an increase in the average impact work KV from 25.71 to 51.05 J, with an average value of BM impact work of 28.09 J.

5. It has been established that welding with a high deposition rate and heat input of $\cong$ 2.2 kJ·mm^{-1} can cause degradation of the CGHAZ metal resistance to brittle fractures under dynamic loads, providing a negative impact on the ballistic resistance and durability of welded joints of the steel. The probable reason for this may be due to the formation of the dominant low-plastic upper bainite structure and the release of boron-containing carbides along the primary grain boundaries, due to the increase in the cooling time of CGHAZ metal from the welding heating temperature.

REFERENCES

1. *U. S. Military Specification MIL-DTL-46100E: Armor Plate, Steel, Wrought, High-Hardness* (U. S. Army Research Laboratory: 2008).
2. S. A. Gladyshev and V. A. Grigoryan, *Bronevyye Stali* [Armour Steels] (Moskva: Intermet Engineering: 2010) (in Russian).
3. O. A. Slyvinskyy, S. P. Bisyk, and K. D. Tonkushina, *Technol. Systems*, **86**, No. 1: 50 (2019).
4. J. A. Garasym, N. A. Bondarevskaya, R. V. Teliovich, V. I. Bondarchuk, V. A. Golub, and S. H. Sedov, *Metallofiz. Noveishie Tekhnol.*, **43**, No. 9: 1235 (2021) (in Ukrainian).
5. H.-R. Lin and G.-H. Cheng, *Mater. Sci. Tech.*, **3**, No. 10: 855 (1987).
6. K. A. Taylor, *Metall. Trans. A*, **23**: 107 (1992).
7. D. T. Llewellyn and W. T. Cook, *Met. Technol.*, **1**, No. 1: 517 (1974).
8. A. Terzic, M. Calcagnotto, S. Guk, T. Schulz, and R. Kawalla, *Mater. Sci. Eng. A*, **584**: 32 (2013).
9. O. A. Gaivoronskyi, V. D. Poznyakov, A. V. Zavdoveyev, A. V. Klapatyuk, and A. M. Denisenko, *The Paton Weld. J.*, No. 5: 3 (2023).
10. W. Pang, N. Ahmed, and D. Dunne, *Australas. Weld. J.*, **56**, No. 2: 36 (2011).

11. T. E. Falkenreck, M. Klein, and T. Böllinghaus, *Mater. Sci. Eng. A*, **702**: 322 (2017).
12. O. Slyvinskyy, Y. Chvertko, and S. Bisyk, *High. Temp. Mater. Proc.*, **23**, No. 3: 239 (2019).
13. B. Savic and A. Cabrilo, *Mater.*, **14**, No. 13: 3617 (2021).
14. M. Zeman, *Weld. Int.*, **23**, No. 2: 73 (2009).
15. I. G. Crouch, S. J. Cimpoeru, H. Li, and D. Shanmugam, *The Science of Armour Materials* (Ed. I. G. Crouch) (Woodhead Publishing: 2017), p. 55.
16. S. J. Manganello and K. H. Abbott, *J. Mater.*, **7**, No. 2: 231 (1972).
17. J. Carrier, E. Markiewicz, G. Haugou, D. Lebaillif, N. Leconte, and H. Naceur, *Int. J. of Impact Eng.*, **104**: 154 (2017).
18. G. P. Anastasiadi and M. V. Sil'nikov, *Rabotosposobnost' Bronevykh Materialov* [Performance of Armor Materials] (Sankt Peterburg: Asterion: 2004) (in Russian).
19. R. L. Woodward, *Int. J. Mech. Sci.*, **20**, No. 9: 599 (1978).
20. S. A. Kotrtechko, Yu. Ya. Meshkov, and R. V. Televich, *Metallofiz. Noveishie Tekhnol.*, **26**, No. 4: 435 (2004) (in Russian).
21. D. Radaj, *Heat Effects of Welding* (Berlin–Heidelberg: Springer-Verlag: 1992).
22. F. B. Pickering, *Fizicheskoe Metallovedenie i Razrabotka Staley* [Physical Metallurgy and the Design of Steels] (Moskva: Metallurgiya: 1982) (Russian translation).
23. R. Celin, F. Kafexhiu, G. Klančnik, and J. Burja, *MTAEC9*, **55**, No. 1: 115 (2021).
24. Z. Zou, Y. Li, and S. Yin, *J. Mater. Sci. Technol.*, **15**, No. 6: 555 (1999).
25. T. S. Prithiv, B. Gault, Y. Li, D. Andersen, N. Valle, S. Eswara, D. Ponge, and D. Raabe, *Acta Mater.*, **252**: 118947 (2023).